IJARCCE ISSN (O) 2278-1021, ISSN (P) 2319-5940

International Journal of Advanced Research in Computer and Communication Engineering

Impact Factor 8.102 ⁜ Peer-reviewed & Refereed journal ⁜ Vol. 13, Issue 2, February 2024

DOI: 10.17148/IJARCCE.2024.13216

IMPLEMENTATION OF THE FORMULATED PELICAN OPTIMIZATION ALGORITHM-BASED INTENSITY HUE SATURATION MODEL USING MATLAB (R2016a) INTEGRATED ENVIRONMENT

Adeyemo Isiaka Akinkunmi[1], Tunbosun Oyewale Oladoyinbo[2], Olabiyisi Stephen Olatunde[3], Ajala Funmilayo Alaba[4]

Department of Computer Science, Ladoke Akintola University of Technology, Ogbomoso, Oyo State, Nigeria[1-4]

iaadeyemo22@lautech.edu.ng

Abstract:

Background: The image fusion model integrates information from two or more images into a single image that is more informative and appropriate for visual perception or computer analysis.

Material and methods: A Samsung 315 digital camera was used to collect the 2,800 datasets, which are photos and postures of randomly chosen students from the Department of Computer Science at Ladoke Akintola University of Technology. The datasets were then normalized to a consistent size of 300 x 300 pixels. Forty percent of the photos were used for testing, and sixty percent of the images were used for training.

Results: The results showed that the EIHS-POA technique has a better performance in accuracy, sensitivity, specificity, precision, and false positive rate than the IHS-POA and POA techniques as enumerated for EIHS-POA datasets, with a recognition accuracy of 96.90%, a sensitivity of 99.37%, a specificity of 92.59%, and a precision of 96.90% compared to the IHS-POA technique, with a recognition accuracy of 95.56%, 97.46% sensitivity, 91.11% specificity, and 96.24% precision. Also, with the EIHS-POA technique, 98.44% of recognition accuracy, 98.41% of sensitivity, 98.52% of specificity, and 99.36% of precision. With the IHS-POA technique, recognition accuracy is 96.44%, with 96.51% of sensitivity, 96.30% of specificity, and 98.38% of precision. The EIHS-POA technique has a lower false positive rate of 7.41%, 5.19%, 2.96%, and 1.48% for enhanced PAN and MULT-SPEC images with recognition times of 100.56s, 101.67s, 107.75s, and 106.97s.

Conclusion: It was concluded that the evaluation obtained in the Enhanced Intensity Hue Saturation Pelican Optimization Algorithm (EIHS-POA)-based procedure had improved high resolution and high visual perception in all instances. The result provided evidence of the importance of applying a Pelican Optimization Algorithm-Based Model to find the high resolution and high visual perception of the system.

Keywords: Enhanced Intensity Hue Saturation Pelican Optimization Algorithm (EIHS-POA), image fusion, pelican optimization algorithm

I. INTRODUCTION

The image fusion model integrates information from two or more images into a single image that is more informative and appropriate for visual perception or computer analysis. Image fusion aims to maximize the relative information unique to a certain application while reducing ambiguity and duplication in the final image (Goshtasby and Nikolov, 2015).

However, algorithms for image fusion fall into three categories: multi-resolution fusion techniques (like Retina-Inspired Model (RIM), wavelets, and Gaussian laplacian pyramid techniques), substitution methods (like principal

International Journal of Advanced Research in Computer and Communication Engineering
Impact Factor 8.102 ⁜ Peer-reviewed & Refereed journal ⁜ Vol. 13, Issue 2, February 2024
DOI: 10.17148/IJARCCE.2024.13216

component analysis and intensity-hue-saturation, or IHS), and arithmetic combination techniques (like Brovey, synthetic variable ratio, and ratio enhancement).

Due to their advantages over other fusion approaches, multi-resolution fusion techniques have been extensively studied in the literature (Tu and Huang, 2007). Based on the biological computations of the human retina, the model was first developed. The three distinct cone cells of the retina, which are sensitive to the short, medium, and long wavelengths of the visible spectrum, work together to enable vision in humans (Ross et al. 2000). Through spatial component processes in its bipolar cells, the outputs from these photoreceptors are contained inside the different bands of the retina. The degree to which a retina can integrate and improve upon the outputs of its photoreceptors will dictate the degree to which a person can recognize objects, particularly those that are colored. However, this study focuses on the implementation of the formulated Pelican Optimization Algorithm-based Intensity Hue Saturation Model using the MATLAB (R2016a) integrated environment.

II. LITERATURE REVIEW

Intensity Hue System Fusion Technique

The IHS spectral transform can successfully convert a multispectral image with red, green, and blue channels (RGB) to IHS spectral space. Among the benefits of IHS transformation operations is the ability to affect each HIS component independently without disturbing the others. This property may be used for the fusion of multi-sensor images. The intensity displays the brightness in a spectrum; the hue is the property of the spectral wavelength; and the saturation is the purity of the spectrum. An intensity image of the IHS system usually looks like a panchromatic image, and this characteristic is used in the image fusion process. The fundamentals of IHS fusion, in summary, are: align the input multispectral image to the panchromatic image if needed; transform the input multispectral image from RGB to IHS color space; substitute the intensity component with a panchromatic image with a higher spatial resolution; and transform the substituted intensity part and original hue and saturation components by reversing to RGB colour space.

This process leads to a fused and enhanced spectral image. Transferring a spectral image from the RGB space to the IHS space is explained by the following equations: Figures 1 and 2 describe the intensity of hue saturation. Algorithm 1 describes the HIS fusion.

$$\begin{bmatrix} I \\ v_1 \\ v_2 \end{bmatrix} = \begin{bmatrix} 1/\sqrt{3} & 1/\sqrt{3} & 1/\sqrt{3} \\ 1/\sqrt{6} & 1/\sqrt{6} & -2/\sqrt{6} \\ 1/\sqrt{2} & -1/\sqrt{2} & 0 \end{bmatrix} \begin{bmatrix} R \\ G \\ B \end{bmatrix} \quad (2.12)$$

$$H = \tan^{-1}\left(\frac{v1}{v2}\right), \quad (2.13)$$

$$S = \sqrt{v1^2 + v2^2}. \quad (2.14)$$

Where $v1$ and $v2$ are the transitional values in equation 2.14. The inverse transformation is described as:

$$v1 = S \sin(H), \quad (2.15)$$

$$v2 = S \cos(H), \quad (2.16)$$

$$\begin{bmatrix} R \\ G \\ B \end{bmatrix} = \begin{bmatrix} 1/\sqrt{3} & 1/\sqrt{6} & 1/\sqrt{2} \\ 1/\sqrt{3} & 1/\sqrt{6} & -1/\sqrt{2} \\ 1/\sqrt{3} & -2/\sqrt{6} & 0 \end{bmatrix} \begin{bmatrix} I \\ v_1 \\ v_2 \end{bmatrix} \quad (2.17)$$

Algorithm 1: IHS Fusion Algorithm

Step 1. Aligning the input multispectral and panchromatic image to the high-resolution image for multispectral image

IJARCCE ISSN (O) 2278-1021, ISSN (P) 2319-5940

International Journal of Advanced Research in Computer and Communication Engineering

Impact Factor 8.102 ⁜ Peer-reviewed & Refereed journal ⁜ Vol. 13, Issue 2, February 2024

DOI: 10.17148/IJARCCE.2024.13216

$$\begin{pmatrix} I \\ v1 \\ v2 \end{pmatrix} = \begin{bmatrix} \frac{1}{\sqrt{3}} & \frac{1}{\sqrt{3}} & \frac{1}{\sqrt{3}} \\ \frac{1}{\sqrt{6}} & \frac{1}{\sqrt{6}} & \frac{1}{\sqrt{6}} \\ \frac{1}{\sqrt{2}} & \frac{1}{\sqrt{2}} & 0 \end{bmatrix} \begin{pmatrix} R \\ G \\ B \end{pmatrix}$$

for panchromatic image

$$\begin{pmatrix} I \\ v1 \\ v2 \end{pmatrix} = \begin{bmatrix} \frac{1}{3} & \frac{1}{3} & \frac{1}{3} \\ \frac{-\sqrt{2}}{6} & \frac{-\sqrt{2}}{6} & \frac{2\sqrt{2}}{6} \\ \frac{-1}{\sqrt{2}} & \frac{-1}{\sqrt{2}} & 0 \end{bmatrix} \begin{pmatrix} R \\ G \\ B \end{pmatrix}$$

Step 2: Transforming the input multispectral image and panchromatic image from RGB to IHS color space For multispectral image

Where $H = \tan^{-1}\frac{v1}{v2}$,

S= $\sqrt{v1^1 + v2^2}$ where $v1$ and $v2$ are the transitional values

For panchromatic image

$$S = 1 - \frac{3min(R,G,B)}{R+G+B}$$

Step 3: Substituting the intensity component with the high-resolution image and transforming the new substituted IHS components into RGB color space. This process leads to a fused and enhanced spectral image For multispectral image

$$\begin{pmatrix} F(R) \\ F(G) \\ F(B) \end{pmatrix} = \begin{bmatrix} \frac{1}{\sqrt{3}} & \frac{1}{\sqrt{3}} & \frac{1}{\sqrt{3}} \\ \frac{1}{\sqrt{3}} & \frac{1}{\sqrt{3}} & \frac{1}{\sqrt{3}} \\ \frac{1}{\sqrt{3}} & \frac{1}{\sqrt{3}} & \frac{1}{\sqrt{3}} \end{bmatrix} \begin{pmatrix} I \\ Ssin(H) \\ S\cos(H) \end{pmatrix}$$

$$I = \frac{R+G+B}{3}$$

$$\begin{cases} H = \frac{G-B}{3I-3B}, S = \frac{I-B}{I}, & if\ B < R, G \\ H = \frac{B-R}{3I-3R} + 1, S = \frac{I-R}{I}, & if\ R < B, G \\ H = \frac{R-G}{3I-3G} + 2, S = \frac{I-G}{I}, & if\ G < R, B \end{cases}$$

The inverse IHS transform is shown below

$$\begin{cases} R = I(1+2S-3SH), & G = I(1-S+3SH), B = I(1-S), & if\ B < R, G \\ R = I(1-S), & G = I(1+5S-3SH), & B = I(1-4S+3SH), & if\ R < G, B \\ R = I(1-7S+3SH), & G = I(1-S), & B = I(1+8S-3SH), & if\ G < R, B \end{cases}$$

IJARCCE ISSN (O) 2278-1021, ISSN (P) 2319-5940

International Journal of Advanced Research in Computer and Communication Engineering

Impact Factor 8.102 ⁜ Peer-reviewed & Refereed journal ⁜ Vol. 13, Issue 2, February 2024

DOI: 10.17148/IJARCCE.2024.13216

For Panchromatic image

$$\begin{pmatrix} F(R) \\ F(G) \\ F(B) \end{pmatrix} = \begin{bmatrix} 1 & \frac{-1}{\sqrt{2}} & \frac{1}{\sqrt{2}} \\ 1 & \frac{-1}{\sqrt{2}} & \frac{-1}{\sqrt{2}} \\ 1 & \sqrt{2} & 0 \end{bmatrix} \begin{pmatrix} Pan \\ v1 \\ v1 \end{pmatrix} = \begin{bmatrix} 1 & \frac{-1}{\sqrt{2}} & \frac{1}{\sqrt{2}} \\ 1 & \frac{-1}{\sqrt{2}} & \frac{-1}{\sqrt{2}} \\ 1 & \sqrt{2} & 0 \end{bmatrix} \begin{pmatrix} 1 + (Pan - 1) \\ v1 \\ v1 \end{pmatrix} = \begin{pmatrix} R + (Pan - 1) \\ G + (Pan - 1) \\ B + (Pan - 1) \end{pmatrix}$$

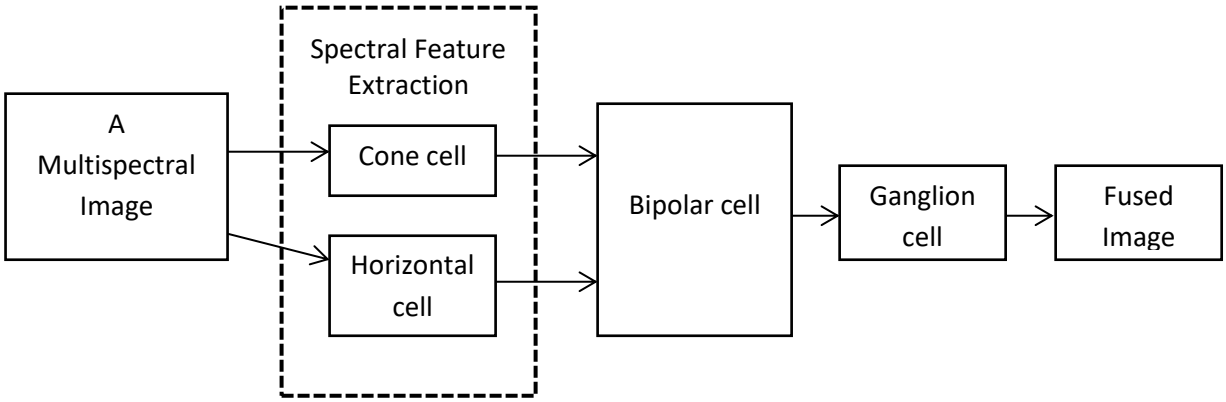

Figure 1: Intensity Hue Saturation.

(Tu and Huang 2007)

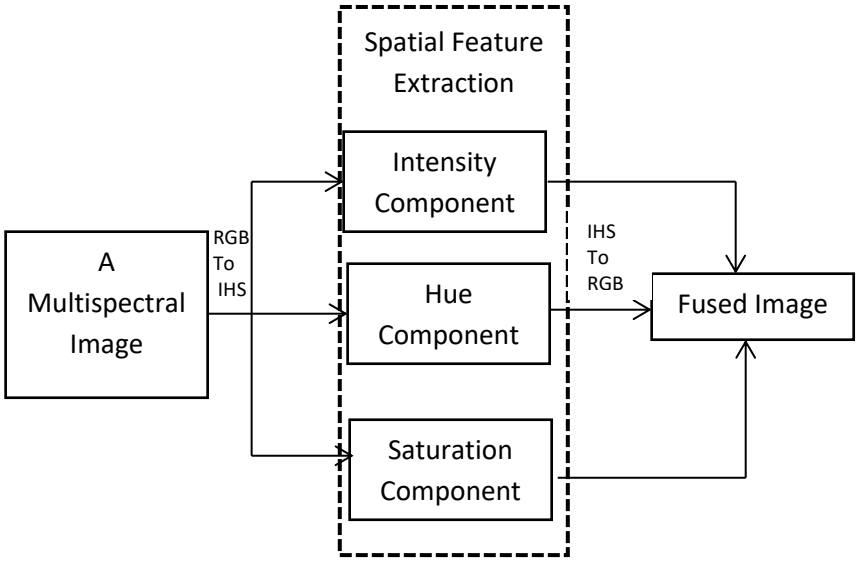

Figure 2: Intensity Hue Saturation.

(Tu and Huang 2007).

Machine Learning Techniques

Different researchers have used machine learning techniques for anomaly detection. Both supervised and unsupervised machine learning techniques can be used to solve several pattern recognition problems (Amusan, Arulogun and Falohun, 2015). Supervised learning is based on using the training data to create a model, in which each of the training

IJARCCE ISSN (O) 2278-1021, ISSN (P) 2319-5940

International Journal of Advanced Research in Computer and Communication Engineering

Impact Factor 8.102 ⁜ Peer-reviewed & Refereed journal ⁜ Vol. 13, Issue 2, February 2024

DOI: 10.17148/IJARCCE.2024.13216

data has a class label. The training stage is to build a classifier model. Once the model is built, it can categorize new instances based on a learned class label. A number of machine-learning-based structures have been used. Some of the machine learning techniques are enumerated in equation 2.18, and their main capabilities and problems are explained for the purpose of this research work. Some of the most common machine learning techniques are Bayesian networks, genetic algorithms (GA), and artificial neural networks (ANN).

Several works have been proposed to change the attributes of intensity hue saturation by introducing optimization models such as kernel principal component analysis, semi-supervised discriminant analysis (SDA), multidimensional scaling, self-organizing maps (SOM), and active shape models for intensity by removing insignificant connections between quantizing the weight, neurons, and intermediate results of IHS.
A number of related studies have been carried out on image fusion using different approaches; some of the areas include security, image processing, and fusion analysis.

Wincy *et al*. (2018) presented a uni-modal and multi-modal biometric identification system for finger knuckle images, palm-print images, and facial images using the SIFT method and the SURF algorithm. They have proposed four techniques, like PROD, MAX, MIN, and SUM methods, to fuse the matching score using a finger knuckle image, a palm-print image, and a facial image. The Max rule has generated maximum accuracy. This multi-modal system using finger knuckle image, palm-print image, and facial image with the SURF method has an acceptance rate of 97.47% and an error rate of 02.52%. The research shows the proposed combination can produce a higher level of security, a lower error rate, and an efficient system.

Tian *et al* (2019) developed a new direction convolution difference vector to efficiently describe the direction details of finger knuckle images. Then, they have also proposed a feature learning method and encoded discriminative direction features for finger knuckle image identification. Final experimental results show that the proposed method outperforms other finger knuckle image recognition techniques, demonstrating the effectiveness of the hash-based methods.

III. METHODOLOGY

A Samsung 315 digital camera was used to collect the 2,800 datasets, which are photos and postures of randomly chosen students from the Department of Computer Science at Ladoke Akintola University of Technology. The datasets were then normalized to a consistent size of 300 x 300 pixels. Forty percent of the photos were used for testing, and sixty percent of the images were used for training.

An image is an array, or a matrix of square pixel (picture elements) arranged in colomns and rows. In an (8-bit) gray scale image each picture element has an assigned intensity that ranges from 0 to 255. A gray scale image is what is usually refered to as a black and white image, but the name emphasizes that such an image also include many shades of gray. A normal gray scale image has 8-bit color depth 256 gray scales. The RGB images of different sizes was first converted to gray-scale where each pixel value is an integer between 0 and 255. These values correspond to the intensity of the pixel where 255 represent the white pixels and 0 represents the black pixel.

The gray-scale images images were normalized to have intensity values of 0 and 1. 0 is assigned to the white (background) and 1 is assigned to the black (see figure 3).

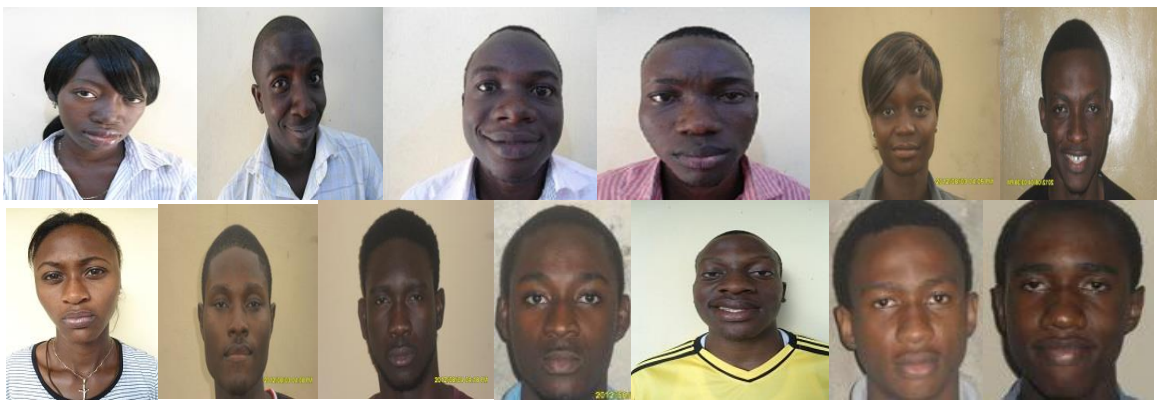

IJARCCE ISSN (O) 2278-1021, ISSN (P) 2319-5940

International Journal of Advanced Research in Computer and Communication Engineering

Impact Factor 8.102 ⁜ Peer-reviewed & Refereed journal ⁜ Vol. 13, Issue 2, February 2024

DOI: 10.17148/IJARCCE.2024.13216

Figure 3: Some Samples of the acquired images

Segmentation of Image

The segmentation of the data was done using Matching Pursuit (MP) algorithm. Matching pursuit (MP) is a sparse approximation algorithm which finds the "best matching" projections of multidimensional data onto the span of an over-complete (i.e., redundant) dictionary '*D*'. The basic idea is to approximately represent a signal 'f' from Hilbert space 'H' as a weighted sum of finitely many functions g_{Yn} (called atoms) taken from '*D*'. An approximation with 'N' atoms has the form

$$f(t) = f_n(t) := \sum_n^N a_n g_{Yn} t \quad (3.1)$$

where g_{Yn} is the Ynth column of the matrix '*D*' and a_n is the scalar weighting factor (amplitude) for the atom g_{Yn}. Normally, not every atom in *'D*' will be used in this sum. Instead, matching pursuit chooses the atoms one at a time in order to maximally (greedily) reduce the approximation error. This is achieved by finding the atom that has the highest inner product with the signal (assuming the atoms are normalized), subtracting from the signal and an approximation that used only that one atom, and repeating the process until the signal is satisfactorily decomposed, i.e., the norm of the residual is small, where the residual after calculating Yn and a_n is denoted by

$$R_{N+1} = f - f_n \quad (3.2)$$

If R_N converges quickly to zero, then only a few atoms are needed to get a good approximation to *f*. Such sparse representations are desirable for signal coding and compression.

Development of Intensity Hue Saturation using IHS-POA

Figures 4 and 5 represent the existing IHS techniques. The framework illustrated in Figure 6 represents the developed enhanced HIS framework for multispectral images. The fused image output of IHS was first converted into a high quality RGB image by employing histogram equalization. Afterwards, the enhanced RGB image will be further

IJARCCE ISSN (O) 2278-1021, ISSN (P) 2319-5940

International Journal of Advanced Research in Computer and Communication Engineering

Impact Factor 8.102 ⁜ Peer-reviewed & Refereed journal ⁜ Vol. 13, Issue 2, February 2024

DOI: 10.17148/IJARCCE.2024.13216

decomposed into its intensity, hue and saturation independent components. Spatial features extracted from these components was fused using wavelet transform. After this, a new intensity image is expected which should contain increased spatial information with increased intensity distribution. Ultimately, the process will be completed by inverse IHS transform of the new intensity and the old hue and saturation components back into RGB space.

Algorithm 4: A pelican IHS fusion

Start POA.
Step 1. Input the RGB color space information.
Step 2. Regulate the POA size of population (N) and the number of repetitions (T).
Step 3. Initialization of the position of pelicans and calculate the objective function.
Step 4. For t = 1:T
Step 5: Generate the position of the prey at random.
Step 6. For I = 1:N
Step 7. Phase 1: Moving towards prey (exploration phase).
Step 8. For j = 1:m
Step 9. Calculate new rank of RGB by inverse transform of the jth dimension using

$$\begin{pmatrix} \boldsymbol{R} \\ \boldsymbol{G} \\ \boldsymbol{B} \end{pmatrix} = \begin{bmatrix} \frac{\mathbf{1}}{\sqrt{\mathbf{3}}} & \frac{\mathbf{1}}{\sqrt{\mathbf{3}}} & \frac{\mathbf{1}}{\sqrt{\mathbf{3}}} \\ \frac{\mathbf{1}}{\sqrt{\mathbf{3}}} & \frac{\mathbf{1}}{\sqrt{\mathbf{3}}} & \frac{\mathbf{1}}{\sqrt{\mathbf{3}}} \\ \frac{\mathbf{1}}{\sqrt{\mathbf{3}}} & \frac{\mathbf{1}}{\sqrt{\mathbf{3}}} & \frac{\mathbf{1}}{\sqrt{\mathbf{3}}} \end{bmatrix} \begin{pmatrix} \boldsymbol{I} \\ \boldsymbol{S}\boldsymbol{sin}(\boldsymbol{H}) \\ \boldsymbol{S}\,\boldsymbol{\cos}\,(\boldsymbol{H}) \end{pmatrix}$$

Where $\boldsymbol{H} = \mathbf{tan}^{-1}\frac{\boldsymbol{v1}}{\boldsymbol{v2}}$,

S= $\sqrt{\boldsymbol{v1^1} + \boldsymbol{v2^2}}$ where $\boldsymbol{v1}$ and $\boldsymbol{v2}$ are the transitional values

$$\boldsymbol{I} = \frac{\boldsymbol{R} + \boldsymbol{G} + \boldsymbol{B}}{\mathbf{3}}$$

$$\boldsymbol{I}, \boldsymbol{H}, \boldsymbol{S}_{i,j}^{\boldsymbol{P1}} = \begin{cases} \boldsymbol{I}, \boldsymbol{H}, \boldsymbol{S}_{i,j} + \boldsymbol{rand}.\left(\boldsymbol{p}_j - \boldsymbol{I}.\left(\boldsymbol{I}, \boldsymbol{H}, \boldsymbol{S}_{i,j}\right)\right), & \boldsymbol{F}_p < \boldsymbol{F}_i \\ \boldsymbol{I}, \boldsymbol{H}, \boldsymbol{S}_{i,j} + \boldsymbol{rand}.\left(\boldsymbol{I}, \boldsymbol{H}, \boldsymbol{S}_{i,j} - \boldsymbol{p}_j\right), & \boldsymbol{else}, \end{cases}$$

where $\boldsymbol{I}, \boldsymbol{H}, \boldsymbol{S}_{i,j}^{\boldsymbol{P1}}$ is the new triangular spectral model of the ith pelican in the jth dimension based on phase 1, I is a random number which is equal to one or two, $\boldsymbol{p}_j$ is the location of prey in the jth dimension, and $\boldsymbol{F}_p$ is its objective function value, F is the objective function vector and $\boldsymbol{F}_i$ is the objective function value of the ith color solution. The parameter I is a number that can be randomly equal to 1 or 2.

Step 10. End.
Step 11. Update the ith population member using

$$\boldsymbol{I}, \boldsymbol{H}, \boldsymbol{S}_i = \begin{cases} \boldsymbol{I}, \boldsymbol{H}, \boldsymbol{S}_i^{\boldsymbol{P1}}, & \boldsymbol{F}_i^{\boldsymbol{P1}} < \boldsymbol{F}_i \\ \boldsymbol{I}, \boldsymbol{H}, \boldsymbol{S}_i, & \boldsymbol{else}, \end{cases}$$

where $\boldsymbol{I}, \boldsymbol{H}, \boldsymbol{S}_i^{\boldsymbol{P1}}$ is the new triangular spectral model of the ith pelican and $\boldsymbol{F}_i^{\boldsymbol{P1}}$ is its objective function value based on phase 1.

Step 12. Phase 2: Winging on the water surface (exploitation phase).
Step 13. For j = 1:m.
Step 14. Calculate new inverse transform of the jth dimension using

$$\boldsymbol{IHS}_{i,j}^{\boldsymbol{P2}} = \boldsymbol{IHS}_{i,j} + \boldsymbol{R}.\left(\mathbf{1} - \frac{\boldsymbol{t}}{\boldsymbol{T}}\right).(\mathbf{2}.\boldsymbol{rand} - \mathbf{1}).\boldsymbol{IHS}_{i,j}$$

where $\boldsymbol{IHS}_{i,j}^{\boldsymbol{P2}}$ is the new status of the ith pelican in the jth dimension based on phase 2, R is a constant, which is equal to 0.2, $\boldsymbol{R}.\left(\mathbf{1} - \frac{\boldsymbol{t}}{\boldsymbol{T}}\right)$ is the neighborhood radius of $\boldsymbol{IHS}_{i,j}$ while, t is the iteration counter, and T is the maximum

IJARCCE ISSN (O) 2278-1021, ISSN (P) 2319-5940

International Journal of Advanced Research in Computer and Communication Engineering

Impact Factor 8.102 ⁜ Peer-reviewed & Refereed journal ⁜ Vol. 13, Issue 2, February 2024

DOI: 10.17148/IJARCCE.2024.13216

number of iterations.

Step 15. End.
Step 16. Update the ith population member using

$$IHS_i = \begin{cases} IHS_i^{P_2}, & IHS_i^{P_2} < F_i \\ IHS_i, & else, \end{cases}$$

where $IHS_i^{P_2}$ is the new status of the ith pelican and $F_i^{P_2}$ is its objective function value based on phase 2.

Step 17. End.
Step 18. Update best candidate solution.
Step 19. End.
Step 20: Output best fused and enhanced spectral image IHS.
End

The enhanced IHS framework for panchromatic images is illustrated in Figure 6. The RGB output of the IHS model was first converted into a panchromatic format; afterwards the quality of the new image was also enhanced using histogram equalization and the computed spatial features was fused using wavelet transform. The resulting image was not pass through the IHS inverse since a panchromatic image is expected. Evaluation of the classifier's performance was done with respect to Sensitivity, Specificity, Accuracy, False Positive Rate, Precision and Computational speed The enhanced model was developed using MATLAB 2016a. The Prgramming language allows plotting of functions and data, implementation of algorithms, creation of user interfaces, and interfacing.

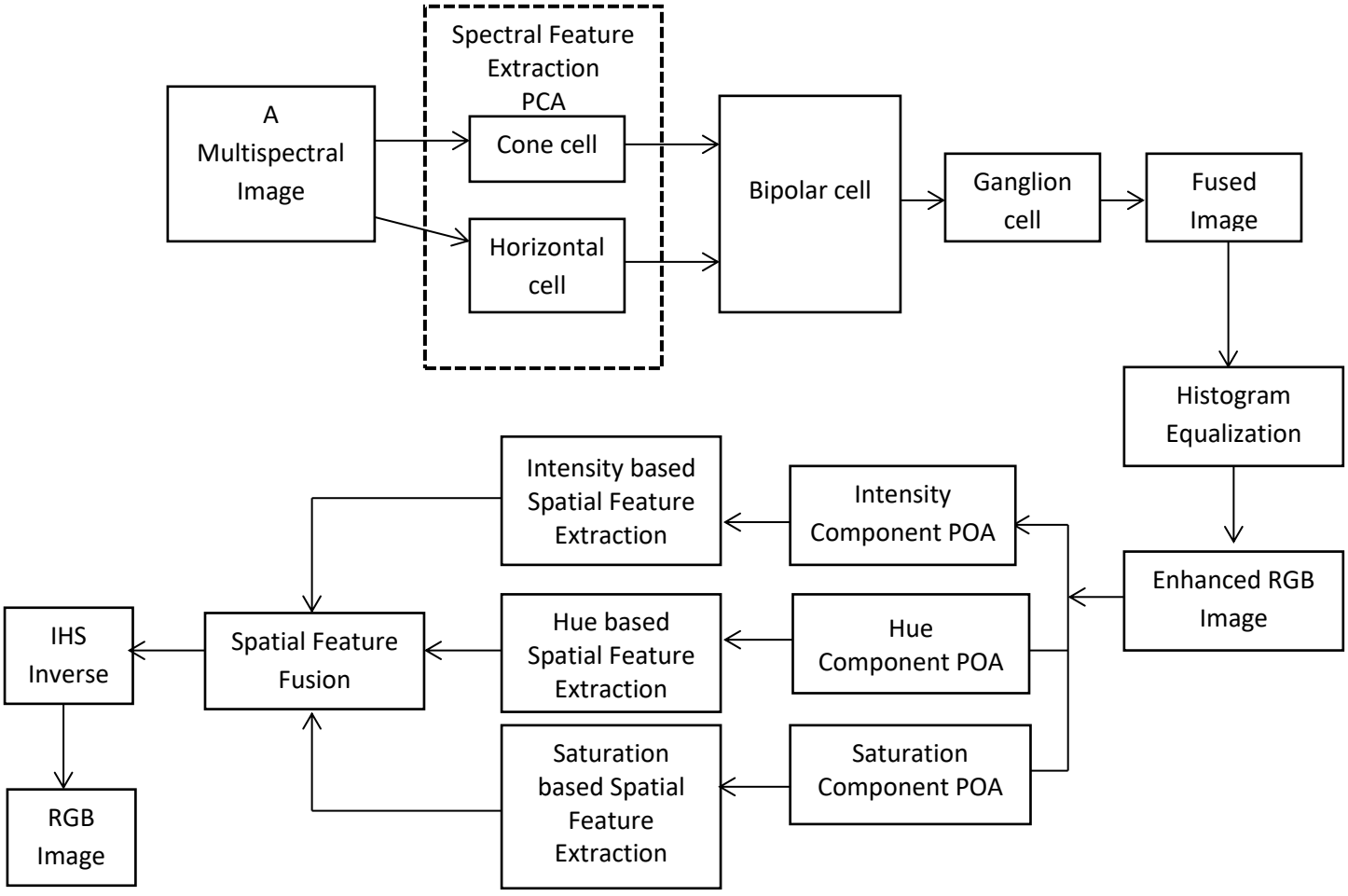

Figure 5: Developed Enhanced IHS for Multispectral Images

IJARCCE ISSN (O) 2278-1021, ISSN (P) 2319-5940

International Journal of Advanced Research in Computer and Communication Engineering

Impact Factor 8.102 ⁜ Peer-reviewed & Refereed journal ⁜ Vol. 13, Issue 2, February 2024

DOI: 10.17148/IJARCCE.2024.13216

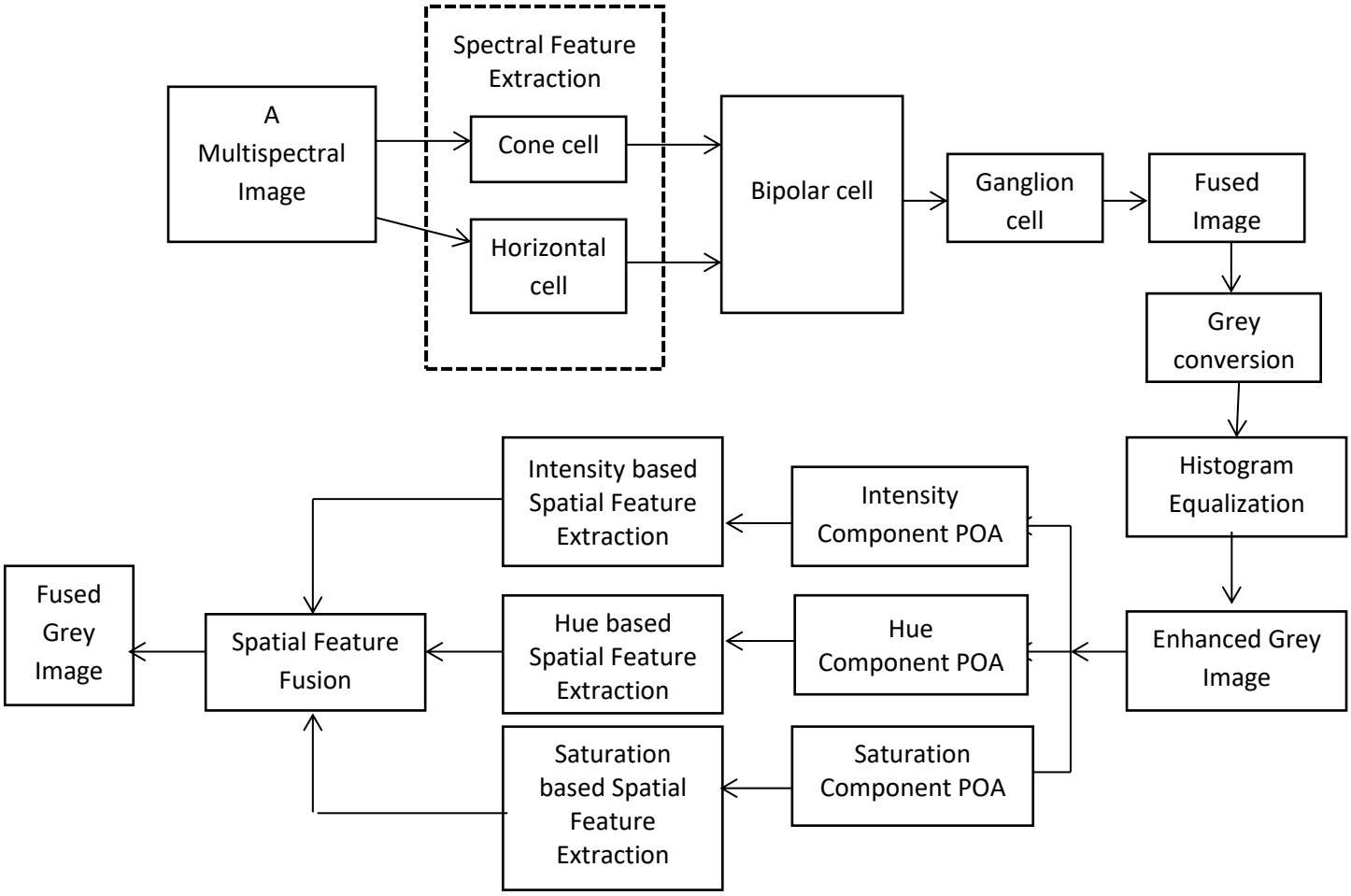

Figure 6: Developed Enhanced IHS for Panchromatic Image

The implementation of the model of the work was done using Matrix Laboratory MATLAB (2016a) software. An interactive Graphic User Interface (GUI) application was developed with an online public database of face dataset. The GUI was also designed using toolboxes such as image processing, computer vision and optimization in MATLAB (2016a).

The MATLAB software package was used for the implementation of a computer system with Intel ® Core™ i7, Windows 10 professional 64-bit operating system, a processing speed of 3.0GHz, 8GB Rando Access Memory (RAM) and 500 GB hard disk drive.

The implementation also allows integration of Pelican optimization application with an existing Intensity Hue Saturation. The developed Intensity Hue Saturation using POA technique was executed using a combination of inputs.

The input was varied to determine the impact of False Positive Rate (FPR), Sensitivity, Computational Time and Precision of the developed technique. The implementation was carried out both interactively and automatically with the following parameters settings according to MATLAB 2016a:

i.20 Virtual Machines (255gb, 512gb, 1000gb of memory)
ii.2000 Number of Tasks
iii.2 Data Centers
iv.Bandwidth (1000mb each)
v.Traffic Type – UDP System used - Windows 10 Ultimate 64-bit operating system, Intel (R) Core ™ i5 Central Processing Unit with a speed of 2.7GH, 4gb Random Access Memory and 500GB hard disk drive.

IJARCCE ISSN (O) 2278-1021, ISSN (P) 2319-5940

International Journal of Advanced Research in Computer and Communication Engineering

Impact Factor 8.102 ⁜ Peer-reviewed & Refereed journal ⁜ Vol. 13, Issue 2, February 2024

DOI: 10.17148/IJARCCE.2024.13216

IV. RESULTS

Table 1 and Table 2 expressed a combined result of IHS, EIHS and EIHS at identifying datasets with respect to the performance metric used for this research. The obtained at optimum threshold of 0.85 in Table 4.7 showed that IHS-POA and EIHS-POA technique has a lower recognition computational time compared with the corresponding EIHS-POA. Similarly, False Positive rate (FPR), Sensitivity, Specificity, accuracy, and computational time of EIHA-POA, IHS-POA were compared; the study discovered that EIHS-POA technique has a better performance in accuracy, sensitivity, specificity, precision, false positive rate than IHS-POA and POA technique as enumerated in Table 2 for EIHS-POA datasets, the recognition accuracy of 96.90%, sensitivity of 99.37%, specificity of 92.59%, and 96.90% precision with IHS-POA technique, recognition accuracy of 95.56%, 97.46% sensitivity, 91.11% specificity and 96.24% precision.

For disguised dataset, the recognition accuracy of 97.78%, sensitivity of 99.05, specificity of 94.81%, and precision of 97.81%, with IHS-POA technique, 95.78% of recognition accuracy, 97.14% of sensitivity, 92.59% of specificity, and 96.84% precision of IHS-POA technique. For other datasets disguised in EIHS-POA, 98.22% of recognition accuracy was discovered, 98.73% of sensitivity, 97.04% of specificity, 98.73% of precision were also reported, with IHS-POA technique, 96.00% of recognition accuracy, 96.83% of sensitivity, 94.07% of specificity and 97.44% of precision were also recognized. Lastly, with EIHS-POA technique, 98.44% of recognition accuracy, 98.41% of sensitivity, 98.52% of specificity and 99.36% of precision. With IHS-POA technique, recognition accuracy of 96.44%, 96.51% of sensitivity, 96.30% of specificity and 98.38% of precision IHS-POA technique.

The EIHS-POA technique has a lower false positive rate of 7.41%, 5.19%, 2.96% and 1.48% for enhanced PAN and MULT-SPEC images with recognition time of 100.56s, 101.67s, 107.75s and 106.97s.

Table 1: Comparison Result of IHS with multispectral image and panchromatic fusion

TP	FN	FP	TN	FPR (%) IHS	SEN (%) HIS	SPEC (%) IHS	PREC(%) IHS	ACC (%) IHS	Time(sec) IHS	Threshold
307	8	12	123	8.89	97.46	91.11	96.24	95.56	120	0.25
306	9	10	125	7.41	97.14	92.59	96.84	95.78	120	0.4
310	10	8	127	5.93	96.83	94.07	97.44	96.00	115	0.6
315	11	5	130	3.70	96.51	96.30	98.38	96.44	112	0.85

Table 2: Comparison Result of EIHS with multispectral image and panchromatic fusion

TP	FN	FP	TN	FPR (%) EIHS	SEN (%) EIHS	SPEC (%) EIHS	PREC (%) EIHS	ACC (%) EIHS	Time(sec) EIHS	Threshold
307	8	12	123	14.81	97.37	92.59	96.90	96.90	100.56	0.25
306	9	10	125	13.33	99.05	94.81	97.81	97.78	101.67	0.4
310	10	8	127	11.85	98.73	97.04	98.73	98.22	107.75	0.6
315	11	5	130	9.63	98.41	98.52	99.36	98.44	106.97	0.85

International Journal of Advanced Research in Computer and Communication Engineering

Impact Factor 8.102 ⁜ Peer-reviewed & Refereed journal ⁜ Vol. 13, Issue 2, February 2024

DOI: 10.17148/IJARCCE.2024.13216

V. CONCLUSION

It was concluded that the evaluation obtained in Enhanced Intensity Hue Saturation Pelican Optimization Algorithm (EIHS-POA) based procedure had an improved high resolution, high visual perception in all instances. The result provided evidence of the importance of applying Pelican Optimization Algorithm based model to find the high resolution and high visual perception of the system.

REFERENCES

[1]. Amusan, D.G., Arulogun O.T. & Falohun A.S. (2015). Nigerian Vehicle License Plate Recognition System using Artificial Neural Network. *International Journal of Advanced Research in Computer and Communication Engineering* Vol. 4, Issue 11.

[2]. Goshtasby, A. S. (2015), "Image fusion: advances in the state of the art", Information Fusion, vol. 8, Issue2, pp. 114–118.

[3]. Ross, W. D. Waxman, A. M. Streilein, W. W. Aguiiar. (2000), "Multi-sensor 3D image fusion and interactive search", Information Fusion, 2000.FUSION 2000. Proceedings of the Third International Conference.

[4]. Tian, C., Zhang, Q., Sun, G., & Song, Z., Li, S. (2019). Fft consolidated sparse and collaborative representation for image classification. *Arab. J. Sci. Eng*. **43**(2), 741–758

[5]. Tu, T. M., Cheng, W.C., Chang, C.P., Huang, P. S., Chang, J.C. (2007). "Best tradeoff for high resolution image fusion to preserve spatial details and minimize color distortion", IEEE Geoscience and Remote Sensing Letters, Vol. 4, Issue 2, pp. 302–306.

[6]. Wincy Anne and Jacob Vetha Raj (2018). A fusion technique for the multimodal biometric system. *International Journal of Computer Sciences and Engineering* 6(2); 492-496.

